

Surface Waves and Scattering and Attenuation

Kiyoshi Yomogida
Professor
Graduate School of Science
Hokkaido University

CONTENTS

Part I. Surface Waves	1
1.1 Love and Rayleigh Waves	1
1.2 Dispersion of Surface Waves	5
1.3 Measurement of Phase and Group Velocities	10
1.4 Estimation of Velocity Structure from Phase (Group) Velocity Observation ...	21
1.5 Regional Variation of Surface Wave Propagation	26
Appendix: Formal Definition of Group Velocity	32
 Part II. Scattering and Attenuation of Seismic Waves	 37
2.1 Coda Waves of Local Earthquakes	39
2.2 Fluctuation of Amplitude and Phase Observed by Seismic Arrays	58
Appendix A: Derivation of Coda Decay Formulation with the Single Scattering Model	 66
Appendix B: Averaged Scattered Wavefield as a Function of Autocorrelation of Velocity Fluctuations	 69
 References	 72

Part II: Scattering and Attenuation of Seismic Waves

First of all, let us compare an ideal model with the actual earth in order to clarify the main goal of the present study.

- { Homogeneous Earth (Lamb's synthetic seismogram in Fig. 2.1)
- { Real Earth (Fig. 2.2)

It is very clear that there is much complexity in any seismogram of the actual earth due to heterogeneities of various scales in the earth. There are two distinct approaches to the study of heterogeneities in the earth:

- Deterministic ... Smoothing out small scale heterogeneities
In this case, we consider heterogeneities only in long-wavelength components compared with the wavelength of seismic waves. Two basic methods (i.e., "tomography" (or travel time inversion) and waveform inversion) have been widely used.
- Stochastic ... Considering all the wavelengths in heterogeneities
Because it is impossible to deterministically match waveforms in the entire frequency range with heterogeneities, we describe them only with small number of statistical parameters of heterogeneities such as mean and variance.

In this part, we shall study the latter case (i.e., stochastic modelling) and review the following two fundamental ways of studying the heterogeneities within the earth :

1. Decay of "coda" wave

Observed seismic waves in general, particularly in records of local events where seismic waves propagate in the shallow part, show remarkable exponential long-tail decay in time, following a P or S wave. Such waves are called "coda" waves, and they are considered to be scattered waves from randomly distributed heterogeneities sampling all the heterogeneities in a given region (Fig. 2.3). Using this coda wave, we may obtain "averaged" characteristics of heterogeneities, which is useful for estimating site, source, and path effects in high frequency.

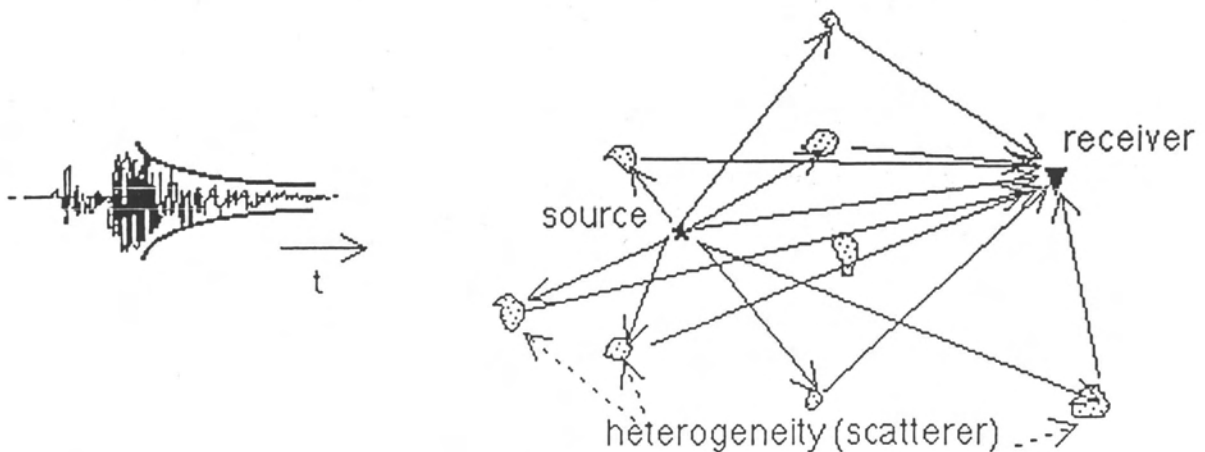


Fig. 2.3: Coda wave of a local earthquake as scattered waves by heterogeneities in the Earth.

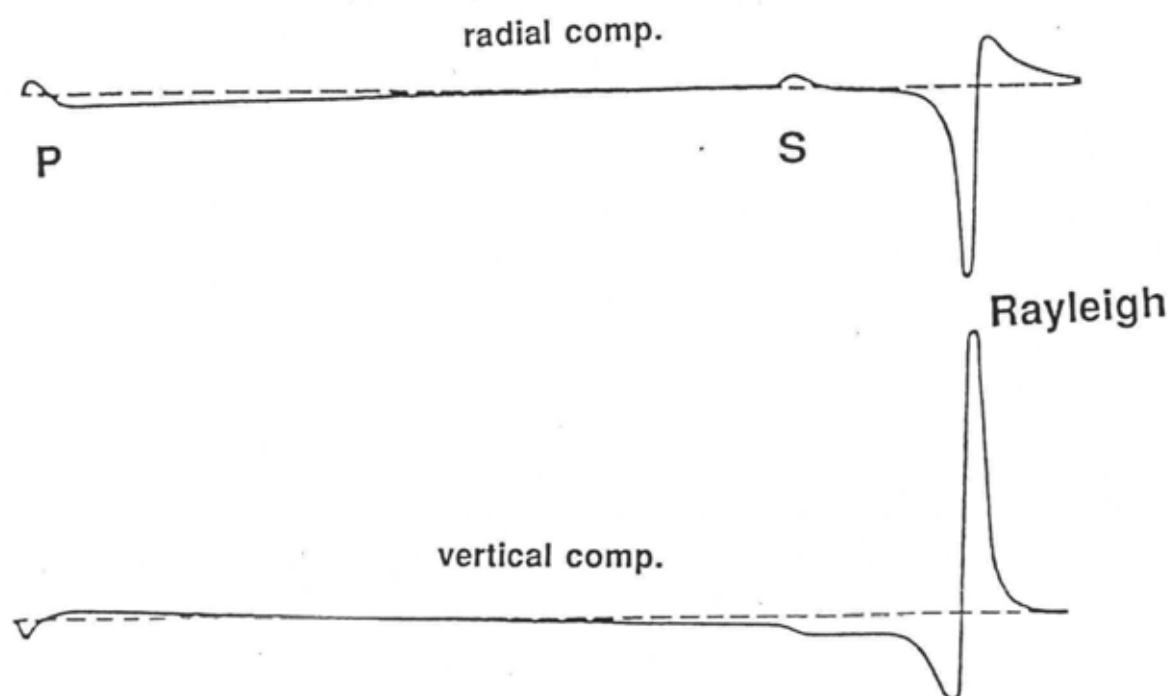


Fig.2.1: Synthetic seismogram by Lamb (1904) for a point force in a homogeneous half space.
 From: Lamb, H., On the propagation of tremors over the surface of an elastic solid, Phil.
 Trans.Roy. Soc. London, A203, 1-42, 1904. (Copyright by Royal Society)

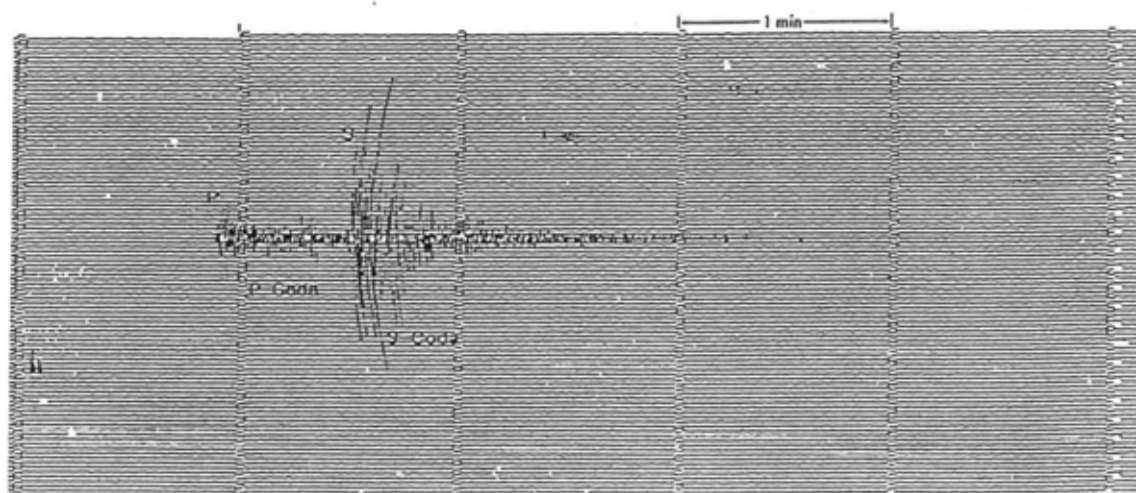


Fig. 2.2: Sample seismogram for a local event recorded in Madrid, Spain, at an epicentral
 distance of 337 km [Herraiz and Espinosa, 1987].

2. Fluctuation of phase delay and amplitude in array observation of teleseismic events

An incident wave having propagated deep in the earth is assumed to have a smooth and coherent wavefront. In such a case, some deterministic approaches are available if we ignore small scale heterogeneities (e.g., three-dimensional travel time inversion). However, once we consider amplitude and phase delay in the high frequency range, observed data is scattered randomly due to complex heterogeneities beneath the array, for example, in the lithosphere (Fig. 2.4).

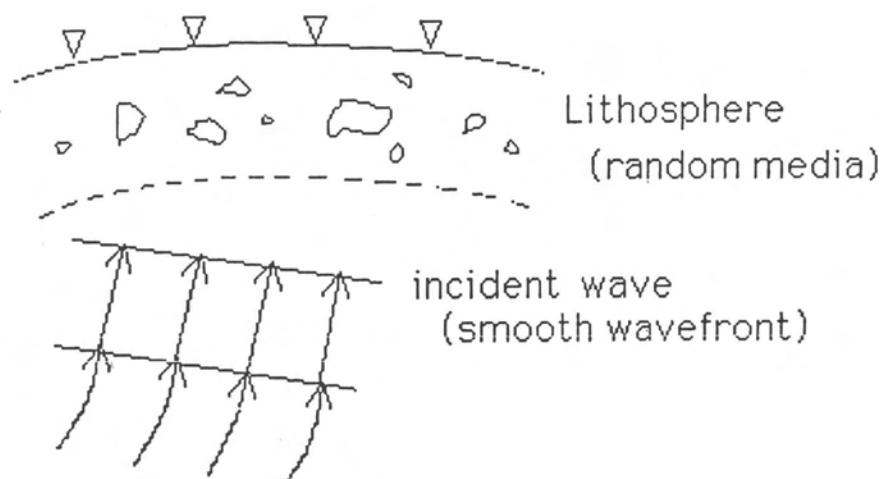


Fig. 2.4: Array observation of a teleseismic event.

An overview of methods in the study of lateral heterogeneities is given in Figure 13.11 of Aki and Richards (1980) and Figures 1 and 2 of Wu (1989). Classifications are made according to two parameters: $ka = 2\pi a / \lambda$ and $kL = 2\pi L / \lambda$ where L is the travel distance, a is the scale length of heterogeneities, λ is the wavelength, and k is the wavenumber (Fig. 2.5). In this part, we shall deal with the right-center part of Fig. 2.5, where any deterministic approaches are impossible.

2.1 Coda Waves of Local Earthquakes

An actual seismogram for a local earthquake generally has the following features (Fig. 2.6):

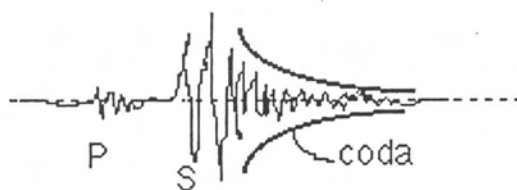
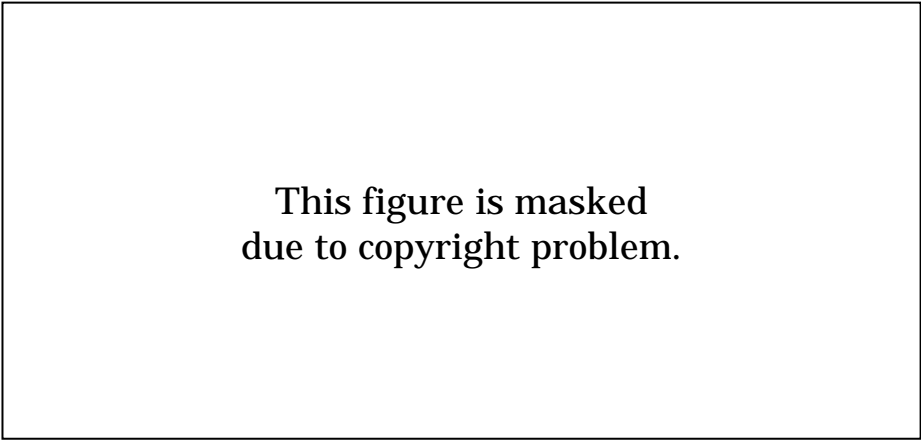


Fig. 2.6: S coda wave.

In addition to P and S waves propagating directly along the path connecting the source and receiver, there is a great amount of energy observed, which decays nearly exponentially over time. Such waves are called coda waves. From various reasons shown later, coda waves, particularly the coda wave which follows a direct S wave, called the S-coda, are considered to be back-scattered S waves of the incident direct S wave due to heterogeneities in the earth. In this note, we shall only discuss the S-coda because the nature of the P-coda, which follows direct P wave, is still controversial.



This figure is masked
due to copyright problem.

Fig.2.5: Classification of scattering problems and applicable methods [after Aki and Richards,1980]. (Copywrite by W.H. Freeman and Company)

Why do we emphasize this kind of wave here? Because of averaging over space, it does not depend on details of path, site, or source effects. We shall discuss the application of coda waves to site (site amplification factor) and source (scaling law) effects later. First, let us summarize some major characteristics of coda waves, as given by Aki and Chouet (1975):

1. While a direct S wave shows complicated variations due to a small change of path, azimuth, focal mechanism, and so on, coda wave spectra are more or less stable.
2. $\Delta < 100$ km (epicentral distance)
A coda duration time is nearly constant regardless of its epicentral distance or azimuth, so it is very useful for estimating the magnitude of an earthquake even if the early part of a seismogram is saturated by strong ground motion.
3. The decay rate of a coda over time is nearly constant regardless of its epicentral distance or azimuth.
4. $M < 6$ (magnitude)
The above item 3 (i.e., coda decay rate) is also independent of the size of earthquakes.
5. The magnitude of coda excitation depends on the surface geology of the recorded site (and earthquake magnitude). Therefore, the coda amplification factor is proportional to the ambient noise at a given site.
6. Array observation of coda waves shows that they come from all directions but not in the specific direction towards source.

What do these characteristics of coda waves mean? They mean that the power spectrum (filtered only around ω) of coda waves at time t can be expressed in general by

$$P(\omega | t) = S(\omega) A(\omega) C(\omega | t)$$

where the term $S(\omega)$ is related to the source, $A(\omega)$ to the site, and $C(\omega | t)$ is independent of either its source or site. In other words, the term $C(\omega | t)$ is invariant inside a given region for all sources and stations, that is, it reflects some intrinsic property of regional structure. It is important that these terms, $S(\omega)$, $A(\omega)$ and $C(\omega | t)$, do not depend on the direction or azimuth connecting the source and receiver, while they are complicated functions of the azimuth in the case of direct P or S waves.

From the above formulation for a coda wave spectrum, we can easily separate each term as follows. Let us consider each term by taking the spectral ratio of two coda records. Take the spectral ratio of coda waves for one earthquake recorded at two stations denoted by 1 and 2,

$$\begin{aligned} \frac{P_1(\omega | t)}{P_2(\omega | t)} &= \frac{S(\omega) A_1(\omega) C(\omega | t)}{S(\omega) A_2(\omega) C(\omega | t)} \\ &= \frac{A_1(\omega)}{A_2(\omega)} \end{aligned}$$

which represents the ratio of site effects between the two stations, 1 and 2. With the use of specific phases such as P and S waves, we must make some precise estimation of the path effect connecting the source and the stations, and the radiation pattern of the source (i.e., azimuthal variation in excitation of these waves). In general, the site effect should depend on the azimuth of incident waves, but in the above formulation with coda waves it represents the mean value over all the directions because of characteristic #6 of coda waves listed above.

Next, let us take the coda spectral ratio for two earthquakes (denoted 1 and 2) observed at one station. We get

$$\begin{aligned}\frac{P_1(\omega|t)}{P_2(\omega|t)} &= \frac{S_1(\omega)A(\omega)C(\omega|t)}{S_2(\omega)A(\omega)C(\omega|t)} \\ &= \frac{S_1(\omega)}{S_2(\omega)}\end{aligned}$$

which represents the ratio of source effects between the two earthquakes. If we use direct arrivals such as P and S waves, we need precise estimation of both path effects and the azimuthal dependency of radiation pattern in order to obtain a reliable comparison of source spectra between two events, which is called the scaling law of sources.

Finally, what does the term $C(\omega|t)$ mean? It reflects the average characteristics of heterogeneities in a given area. Empirically, its power spectral can be expressed by

$$C(\omega|t) = Bt^{-m} \exp\left(-\frac{\omega t}{Q(\omega)}\right).$$

$m \approx 2$ for most observations. This parameter is not as critical as the exponential term. $Q(\omega)$ is the primary parameter to describe the decay rate of coda waves over time (Fig. 2.7).

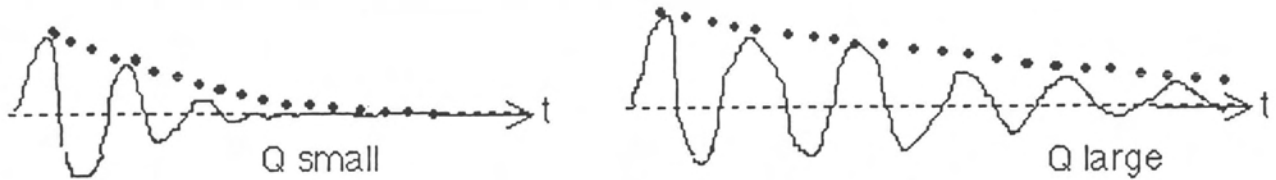


Fig. 2.7: Coda Q.

The most important conclusion from these observations is that the parameter $Q(\omega)$ is nearly constant over a given area, probably up to the scale length of 100 km. In other words, the value of $Q(\omega)$, called the coda Q , can be considered as one of characteristic parameters in representing the structure of the area. This value probably includes both scattering and intrinsic (i.e., anelastic) attenuation effects, as expressed by $Q^{-1} = Q_s^{-1} + Q_i^{-1}$ where Q_s and Q_i represent attenuations due to scattering and the anelasticity of media, respectively. It is, however, still controversial whether the above formulation of the coda Q is valid or not. In Appendix A, the formulation of $C(\omega|t)$ is derived, assuming that the scattering of each wavepacket occurs only once during its propagation from source to receiver, which is called the single scattering model (Aki and Chouet, 1975). Although several other theories have been proposed for the temporal change of coda waves, please refer Appendix A if you are interested in some theoretical background of the formulation of $C(\omega|t)$.

(a) Stability of Coda Q

Now, we shall look through several important results obtained from coda wave analyses. As mentioned above, the time decay rate of coda waves or the coda Q is unique within a given area regardless of stations or events. A clear example of this is in Aki (1969) for two aftershocks of the Parkfield earthquake in California in 1966. Fig. 2.8 shows two sets of vertical seismograms recorded at stations #1 and #9. Each station consists of two kinds of records: high and low gains. In the upper example the source is close to station #1 while it is close to station #9 in the lower. Later parts of the seismograms or coda parts are surprisingly similar to each other, independent of source and station, although early parts are completely different from each other. This example clearly shows how stable the temporal decay of coda waves is in a given area. In measurement of the coda Q , we do not therefore need to worry about either source location, focal mechanism, or site condition.

A similar example is shown in figures of Rautian and Khalturin (1978) who studied seismograms recorded in Garm, Tadjikistan (former USSR). They designed a set of filtered seismograms with several frequency bands in the range of 0.07 to 18 Hz. Fig. 2.9 shows five band-passed seismograms at one station for one event (note that the time axis of their records is opposite to our normal convention). Fig. 2.10 shows the envelopes of these seismograms for various earthquakes in the diagram of amplitude logarithm versus time logarithm. In the earlier sections, the size of the envelopes depends on both the magnitude and epicentral distance of the events. In contrast, they start to converge into one decay curve characteristic in each frequency band as the time lapses. They seem to be sufficiently converged after twice the direct S wave travel time has elapsed.

Fig. 2.11-13 are taken from Aki and Chouet (1975) for similar seismograms recorded in the Kanto area, Japan and in the NORSAR array, Norway. Fig. 2.12 shows coda amplitude versus log time diagrams. It is also clear from these figures that the temporal decay rate of coda waves is nearly constant irrespective of either source or station, and it is dependent only on the frequency considered.

All the above examples prove the remarkable stability of the coda Q , which can be considered to depend only on frequency within a certain area. In Fig. 2.14, incoherency of coda waves is clearly presented with an array observation [Scheimer and Landers, 1974]. This example was recorded at LASA (a big seismometer array) in Montana, U.S.A., in a frequency band of 1 to 2 Hz. This figure shows the wavenumber diagram, which gives the direction and phase velocity of the incoming wave energy, for both the part just after S wave and the later part with the coda waves. In the former, all the energy comes from a specific direction, nearly from west, with the phase velocity of 3.5 km/s, which corresponds to the direct S wave while energy seems to come in all the directions in the latter case. In other words, the S wave comes from a single path connecting source and receiver while coda waves are nearly incoherent, coming from everywhere. This example clearly demonstrates that coda waves sample all the regions in a considered area, giving a number which reflects the average characteristics of the heterogeneities in that area.

(b) Regional Variation of Coda Q^{-1}

Once the coda Q^{-1} was proven to give a representative value of the heterogeneities in a certain area, many researchers have measured it at many places around the world. Although their primary goal was to obtain the value of attenuation factor (i.e., Q_b^{-1} for S wave) of seismic waves such as P and S waves, such estimation is extremely difficult particularly in high frequency range because of complex path and source effects involved as mentioned before. So, they have used coda waves to estimate attenuation factors of seismic waves instead. Fig. 2.15 schematically summarizes those studies: the coda Q , Q_c^{-1} , versus frequency diagram, both in logarithmic scale. We also show spatial variations of coda Q^{-1} in Japan and U.S.A. (Fig. 2.16 and 2.17).

For example, seismograms recorded in the eastern U.S.A. always show a long duration of coda waves or the attenuation of each phase is very small as a function of epicentral distance. In contrast, coda duration time

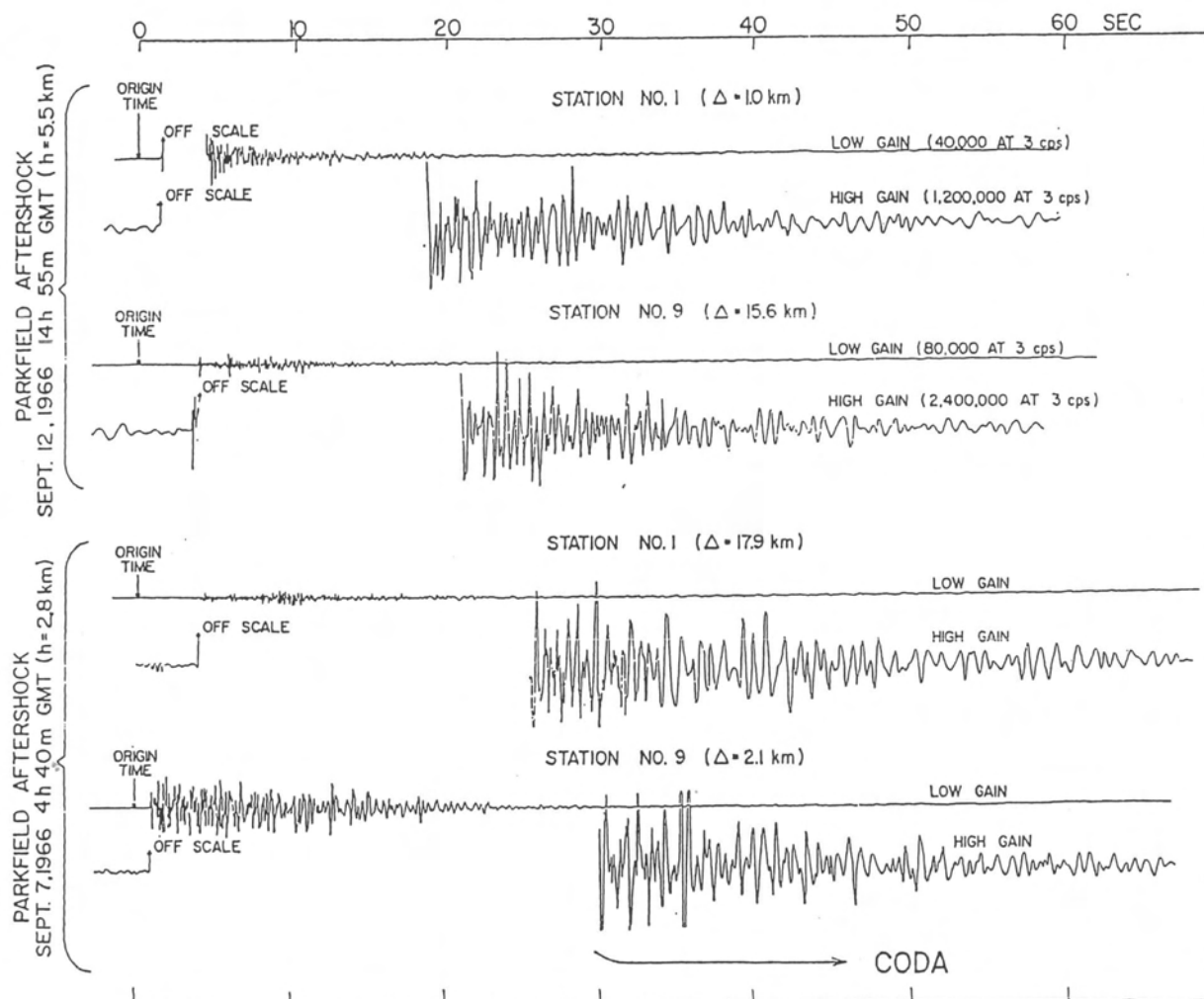


Fig. 2.8: Vertical seismograms of two aftershocks of the Parkfield, California, earthquake in 1966 recorded at two nearby temporary stations [Aki, 1969]. (Copyright by the American Geophysical Union)

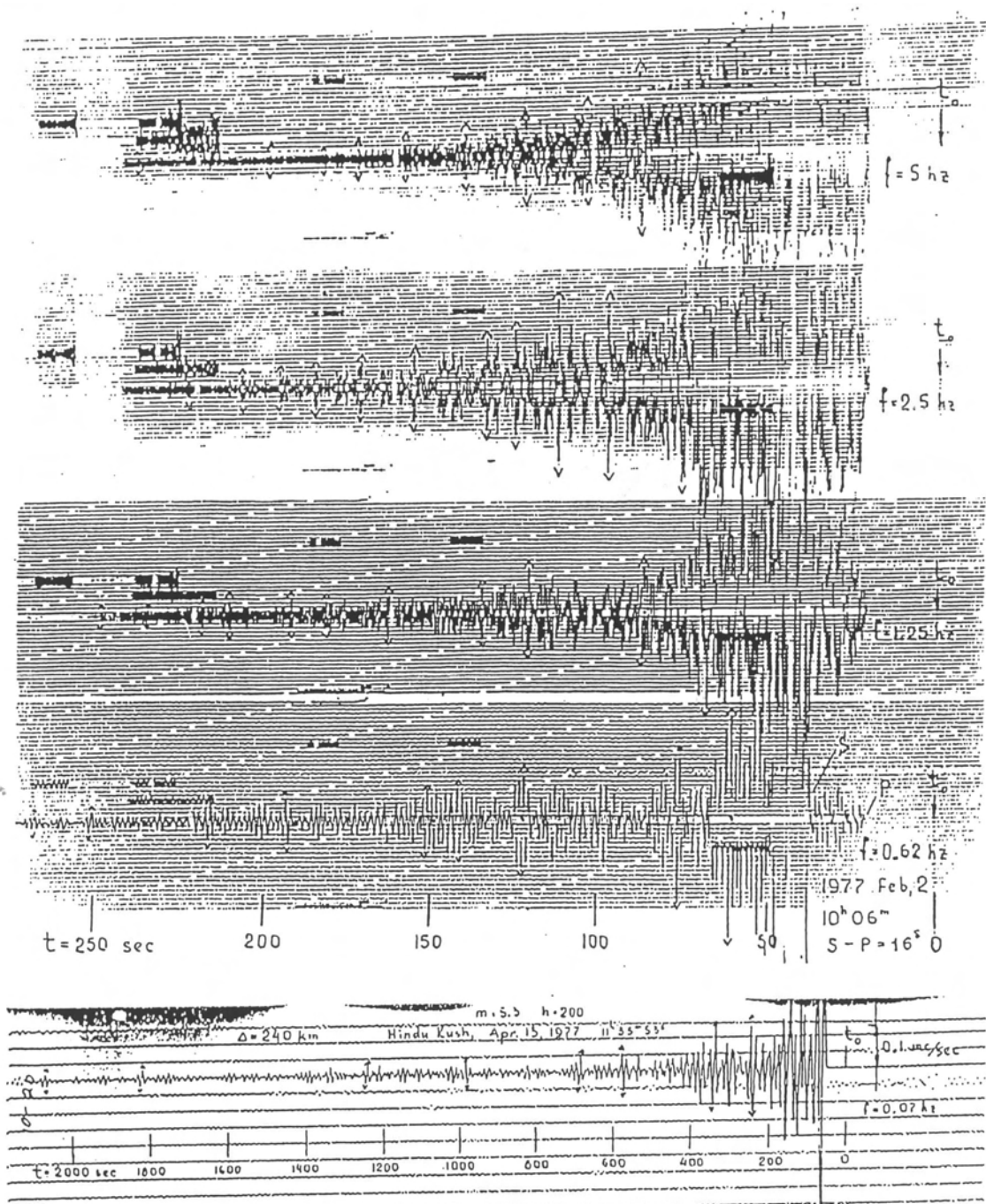


Fig. 2.9: Seismograms in five frequency bands for a local event recorded in Garm, Tadjikistan [Rautian and Khalturin, 1978].

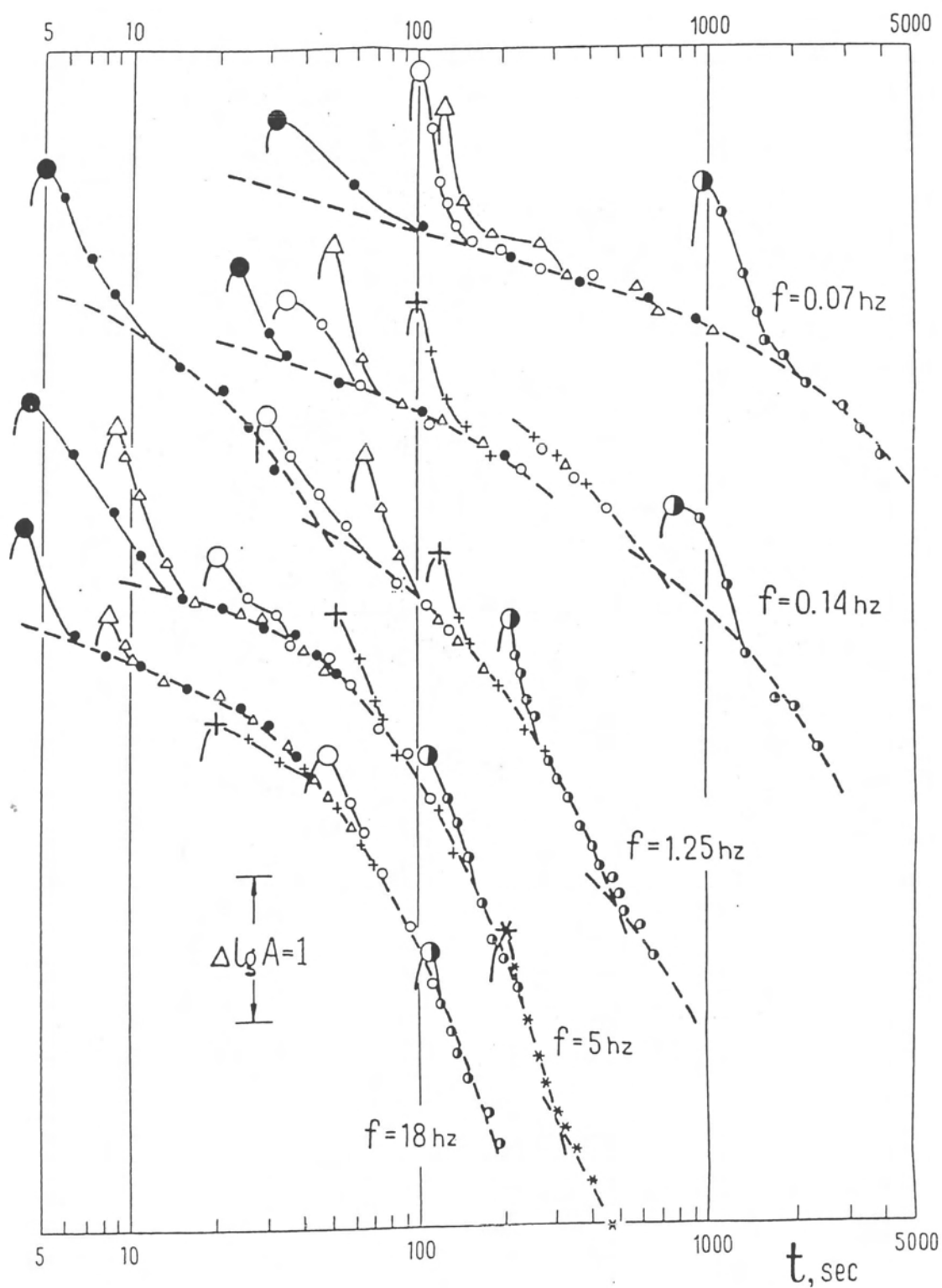


Fig. 2.10: Coda envelopes in five frequency bands for various events recorded at the station of Fig. 2.9 [Rautian and Khalturin, 1978].

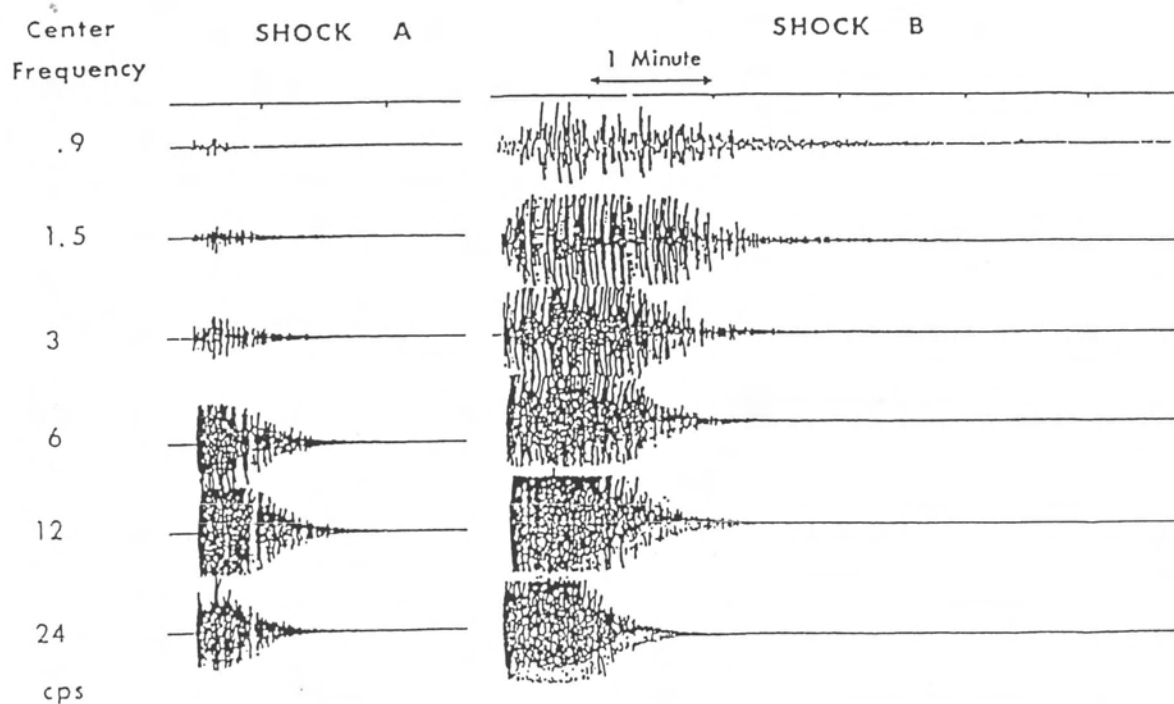
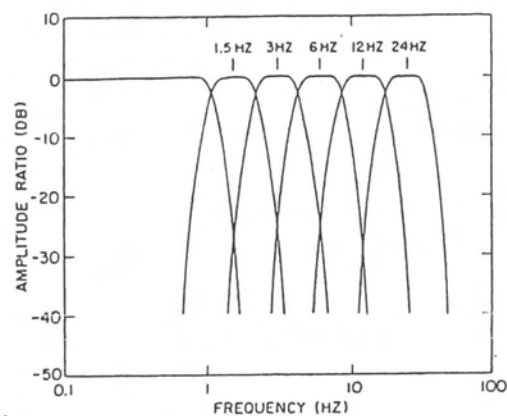
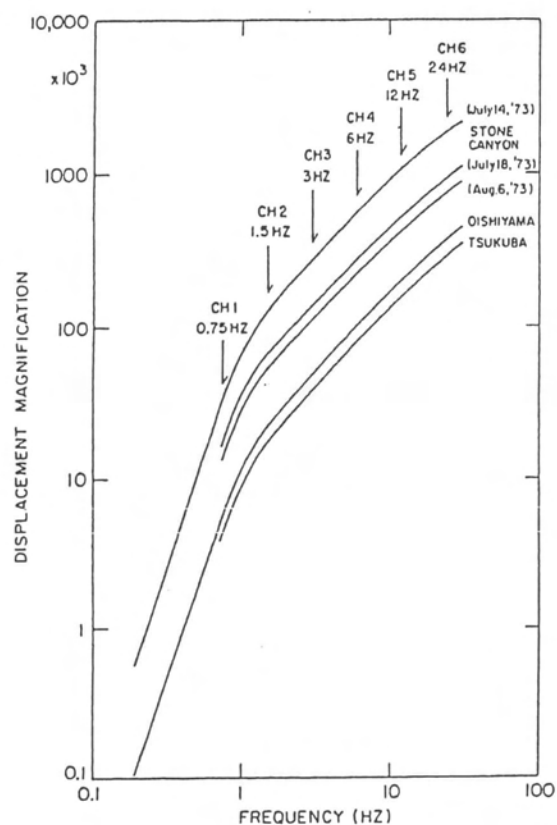


Fig. 2.11: Frequency response curves of bandpass filters and their seismograms recorded at Tsukuba, Japan [Aki and Chouet, 1975]. (Copyright by the American Geophysical Union)

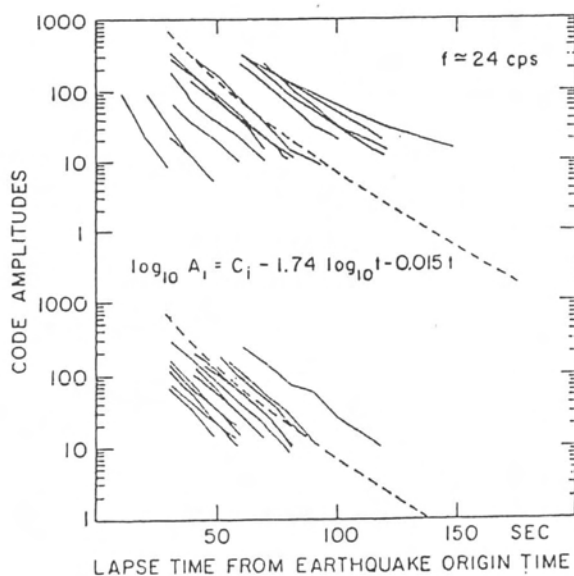
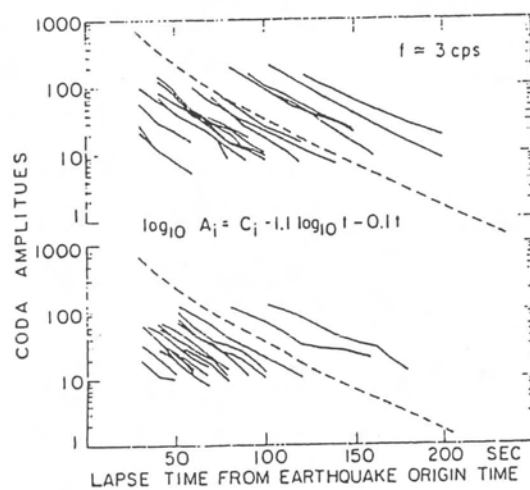
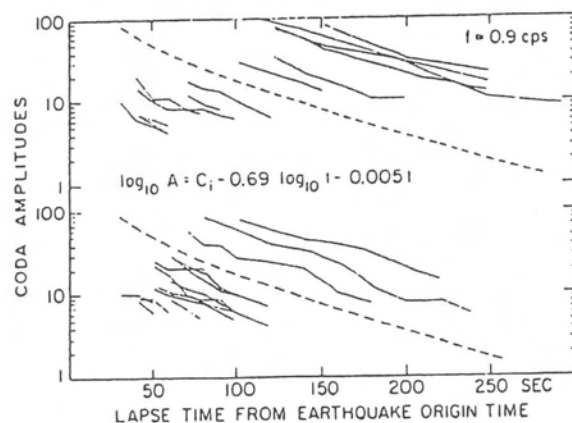


Fig. 2.12: Amplitude decay traces of coda waves in three frequency bands [Aki and Chouet, 1975]. (Copyright by the American Geophysical Union)

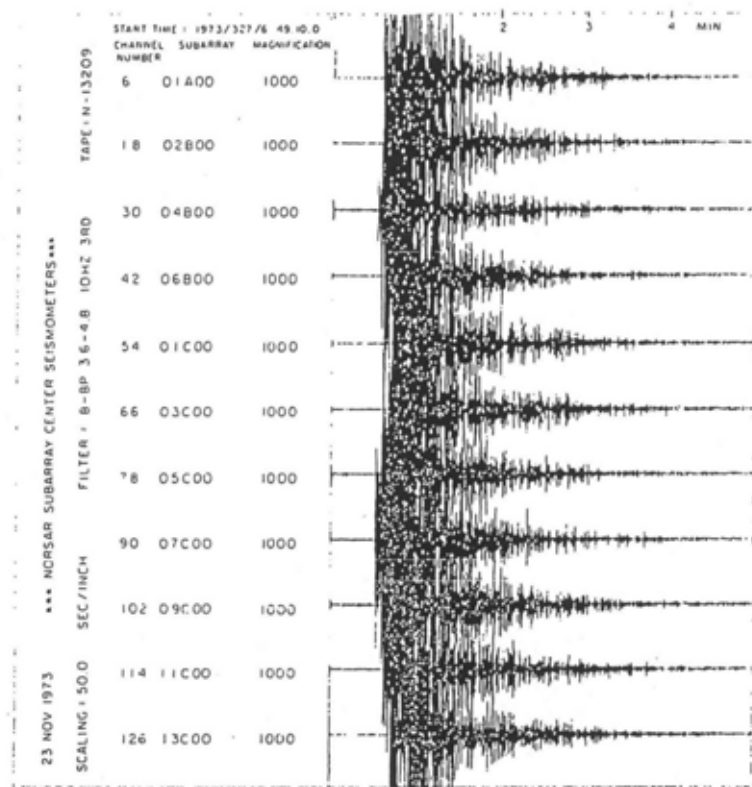


Fig. 2.13: Short-period seismograms of a local earthquake recorded at the NORSAR array in Norway [Aki and Chouet, 1975]. (Copyright by the American Geophysical Union)

This figure is masked
due to copyright problem.

Fig.2.14: Wavenumber spectrals for S arrival and S coda recorded at the LASA array in Montana, U.S.A. [Scheimer and Landers, 1974]. (Copywrite by Massachusetts Institute of Technology)

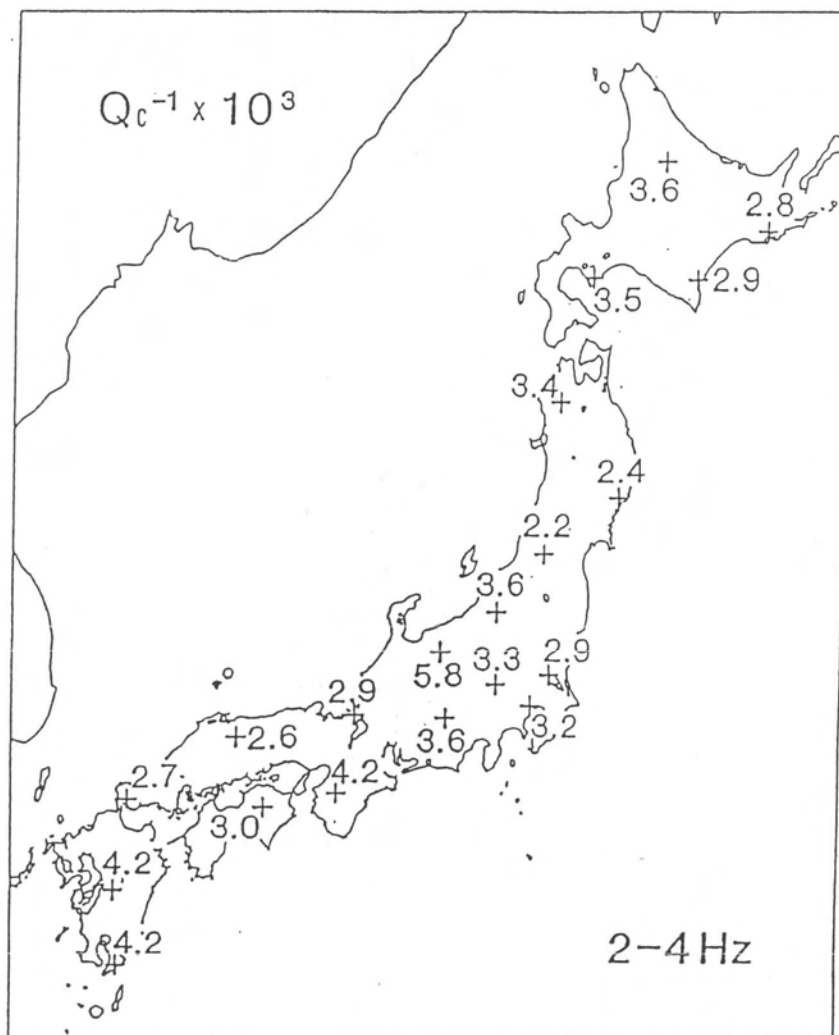


Fig. 2.16: Spatial variation of coda Q in Japan [Hoshiba and Goto, 1988].
(Copyright by the Seismological Society of Japan)

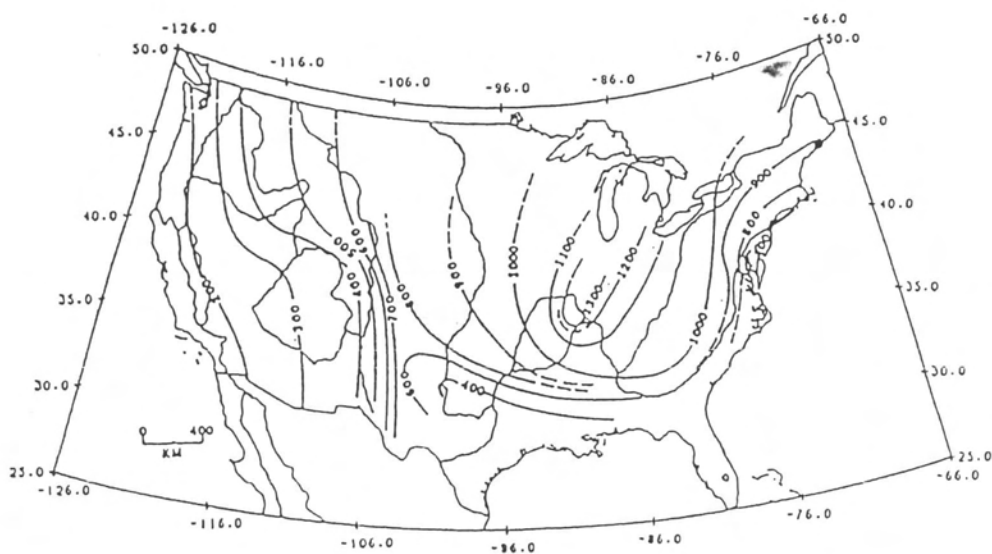


Fig. 2.17: Spatial variation of coda Q at 1 Hz in U.S.A. [Singh and Hermann, 1983].
(Copyright by the American Geophysical Union)

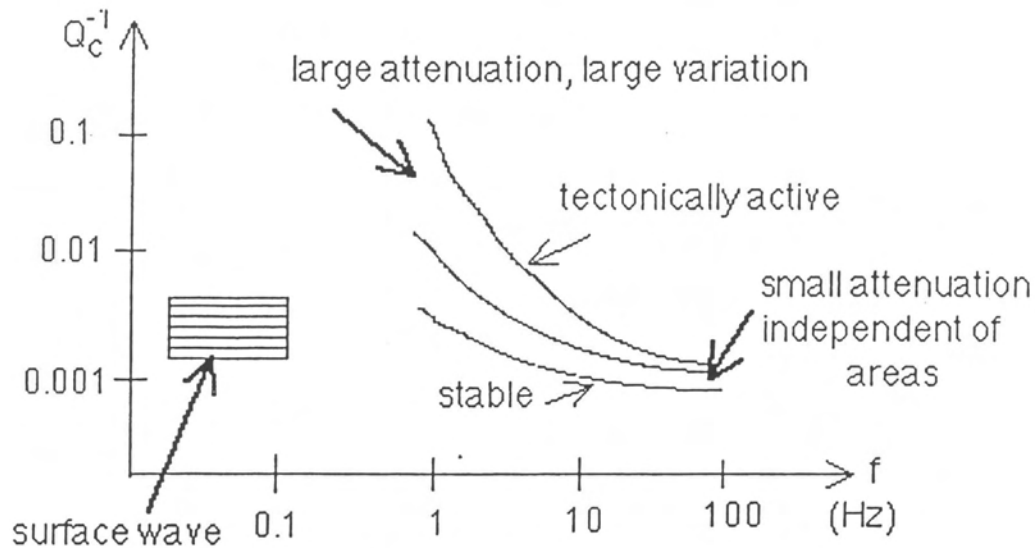


Fig. 2.15: Schematic diagram of frequency dependent Q .

is much shorter and apparent attenuation is much larger in the western U.S.A. This difference implies that the spatial distribution of ground motion is quite different from one region to another even for earthquakes of the same size, which should be very important in making a reasonable estimate of earthquake magnitude or eventually related earthquake hazard.

Spatial variation of coda Q^{-1} also varies in frequency (Fig. 2.18): in a high frequency range, say higher than 10 Hz, there is no great difference in its value around the world while large regional variations are observed at around 1 Hz. This might imply that regional variations in crustal heterogeneities are the strongest in the corresponding size (~several km) of this frequency range, compared with other sizes. Q_c^{-1} values therefore seem to reflect tectonic characteristics: large in tectonically active areas such as orogenic belts and fault zones and small in stable parts of continents such as Pre-Cambrian shields. Since the coda wave is the only tool for making good estimation of the attenuation characteristics of seismic waves in the high frequency range, more careful study should be conducted in this research field.

(c) Site Effects

Next, let us look at the usefulness of coda waves in estimating complex site effects in the high frequency range. Let us look at one clear example given by Tsujiura (1978) who measured site amplitude ratios between two stations using both direct S waves and coda waves (Fig. 2.19). Using one station as a reference site, site amplitude ratios at three stations are estimated in six frequency bands (0.75 to 24 Hz) for many earthquakes propagating to the stations with various incident angles. Estimated values are very stable with the coda waves while scattering in the ratios among different events is large with direct S waves. Since S waves arrive in one particular direction, site amplification factors which depend on complex surface geology under the station should be a sensitive function of incident azimuth. On the other hand, because coda wave energy comes nearly uniformly from all directions, the ratio estimated from coda waves is expected to represent the average site effect over waves coming from all directions. Indeed, the frequency dependency of each site effect estimated from coda waves agrees well with the average values estimated from direct S waves. Coda waves are therefore useful in obtaining the average characteristics of a given site.

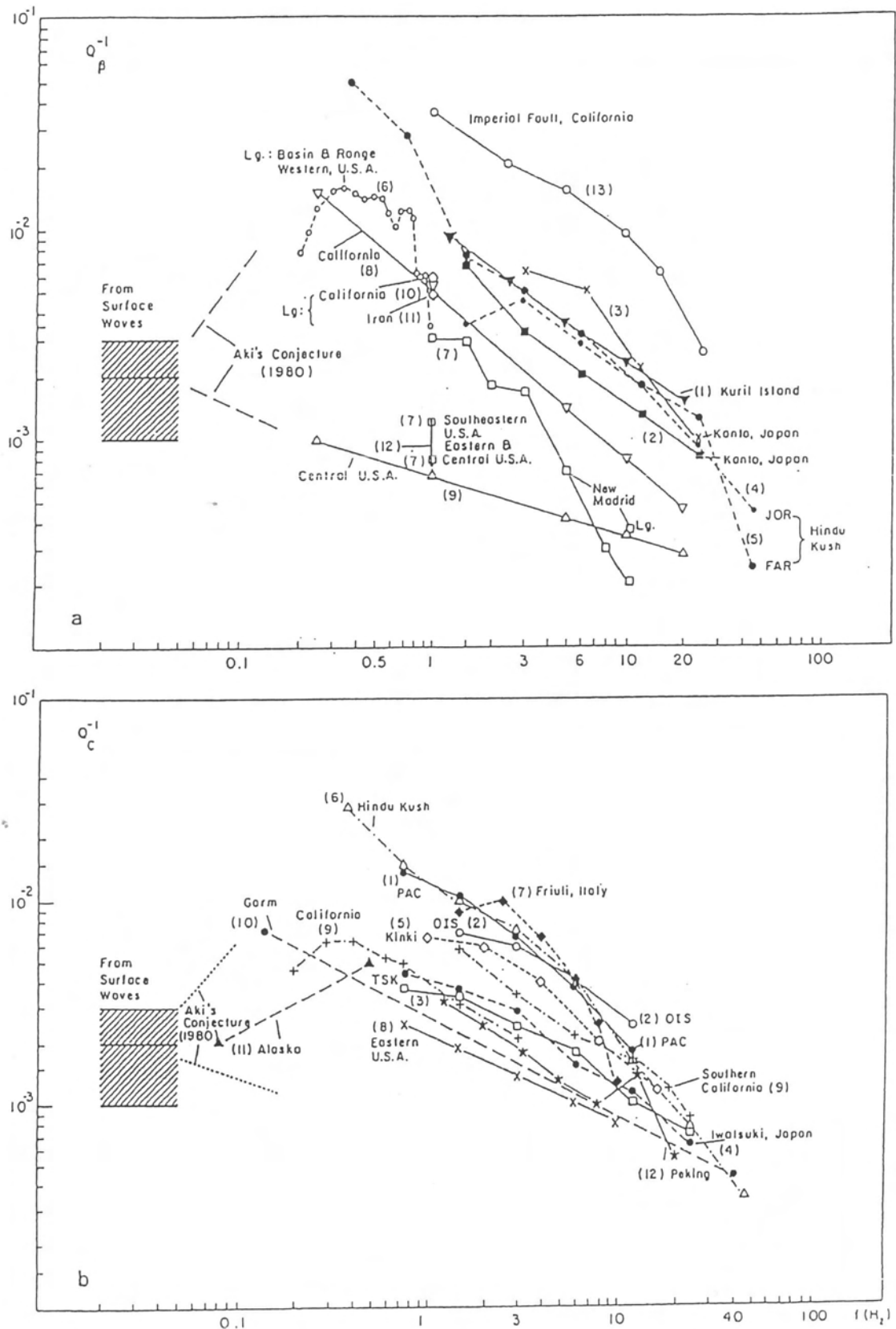


Fig. 2.18: Summaries of S wave Q and coda Q in various areas [Wu, 1989].
(Copyright by Van Nostrand Reinhold)

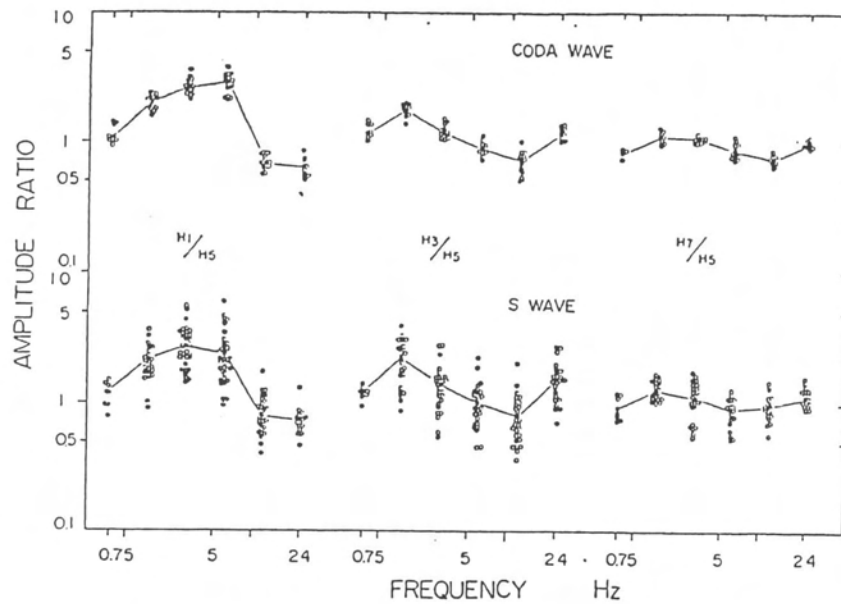


Fig. 2.19: Amplitude ratios of S and coda waves of three stations as a reference of one station (H5) at Dodaira, Kanto [Tsujiura, 1978].

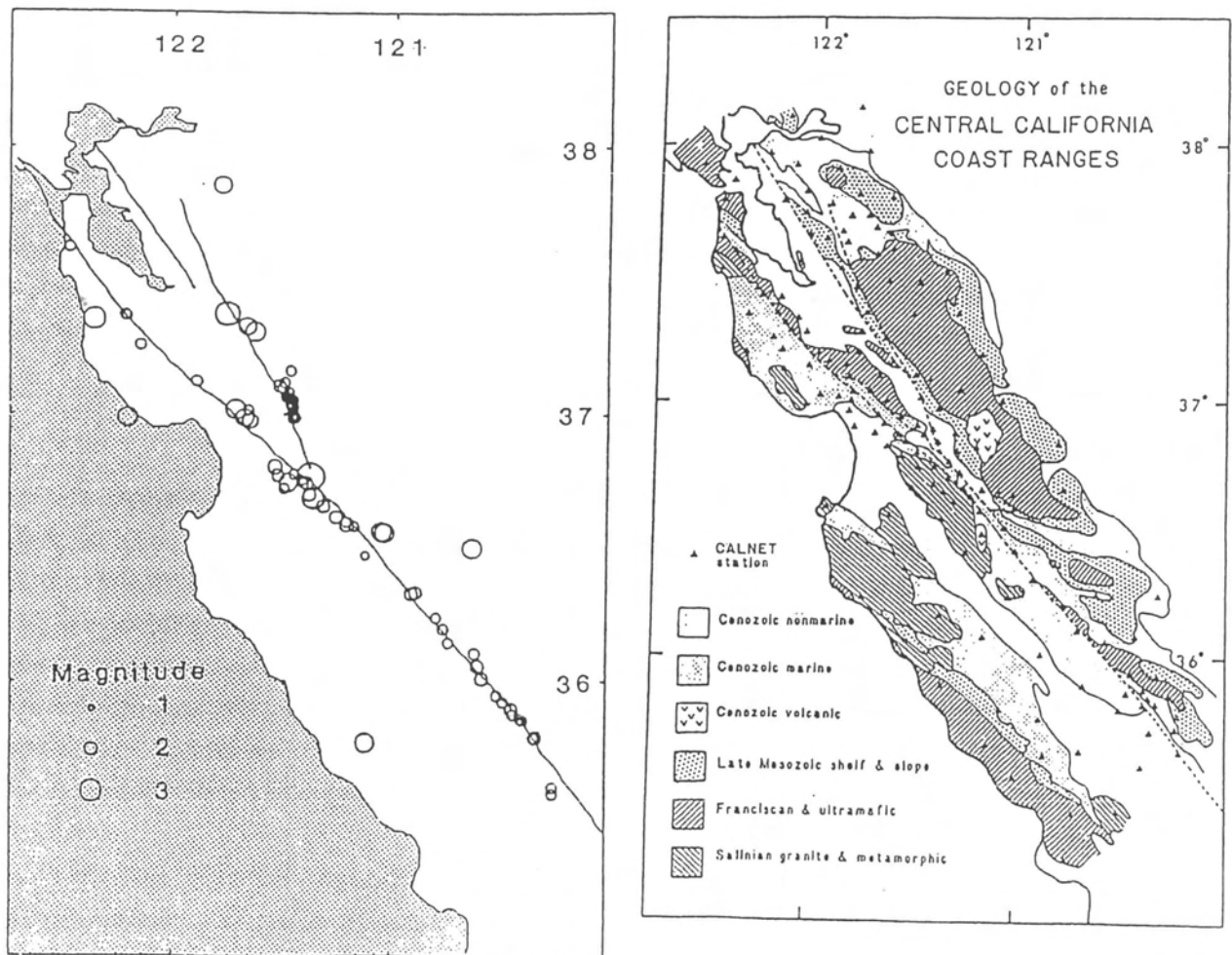


Fig. 2.20: Epicentral distribution and surface geology near the San Andreas fault in central California [Phillips and Aki, 1986].

The next example is taken from Phillips and Aki (1986) who studied site amplification factors quantitatively, using the important feature of coda waves mentioned above with the Central California seismic network of the U.S. Geological Survey (Fig. 2.20-22). As we discussed before, the power spectral of coda waves $P(\omega, t)$ can be expressed by

$$\frac{1}{2} \ln P_{ij}(\omega_l, t_k) = d_{ijkl} = r_i(\omega_l) + s_j(\omega_l) + c(\omega_l, t_k)$$

where i, j, k , and l denote the site, the source, the time, and the frequency indices, and r_i, s_j and c are the site term, the source term, and the term independent of source and site locations, respectively. Let us remember that with the single scattering model

$$c(\omega, t) \propto -2 \ln t - \omega t / Q_c(\omega)$$

does not depend on either source j or site i . For each frequency band l , we can get the following formulation with each observation site i :

$$d_{ijk} - \bar{d}_{jk} = r_i - \bar{r}_{jk}$$

where each value with a bar represents the average over all the sites i with a fixed source j and a lapse time k .

Fig. 2.21 shows site response maps or variations of $r_i(\omega)$ at each site from the average values obtained from the above formulation at frequencies of 1.5 and 12 Hz. Fig. 2.22 shows scattering in data for site amplification factors as a function of frequency with different surface geological regions such as granite, fault zone, Franciscan, and sediment. In the low frequency range, the amplification factor is large for granite sites, while the tendency is reversed or the factor becomes larger for fault zones than for granite sites in the high frequency range although scattering in data is quite large for granite sites. More precise study on site amplification factors using the present technique might be extremely useful in estimating the damage caused by large events around a given area.

(d) Source Effect: Scaling Law

One of the most important subjects in seismology is the estimation of average frequency spectra radiated by earthquakes as a function of their size or magnitude. The following diagram shows a typical relationship between radiated source spectra versus frequency, implied from some theoretical approaches and estimated from very careful measurement of actual earthquakes. Such a relationship is called the "scaling law" of seismic sources. This kind of measurement is extremely difficult because such estimations are affected by minute variations, for example, in the radiation pattern of the source and any complex path effects, particularly in the high frequency range. Such a scaling law could be obtained from a set of earthquakes with different magnitudes occurring at a similar location and with a similar focal mechanism recorded at one station, in order to minimize the above factors (Fig. 2.23).

In low frequencies, radiated energy is relatively flat in spectrum, or frequency independent and proportional to the size of earthquakes. On the other hand, the frequency spectrum decreases as a function of nearly ω^{-2} in the high frequency range with the "corner frequency" which depends on its magnitude. This drop in the high frequency spectrum is mainly due to the finiteness of the source dimension and source time function.

Scaling laws in Fig. 2.24 and 2.25 are taken from Rautian and Khalturin (1978) and Aki and Chouet (1975). With several minor corrections, these source spectrals are estimated from coda waves but not direct P or S

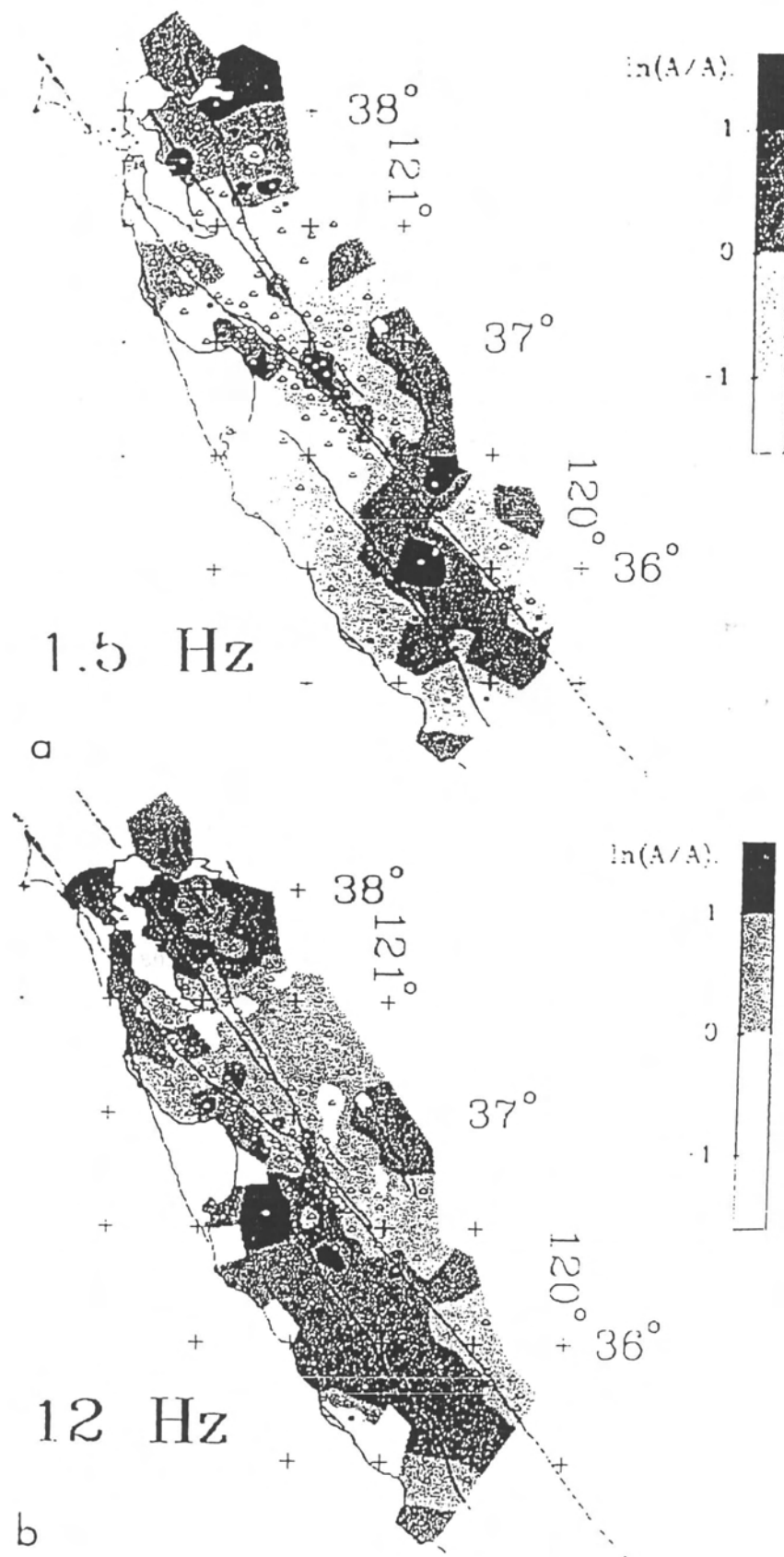


Fig. 2.21: Site response maps obtained from coda wave in two frequency bands [Phillips and Aki, 1986].

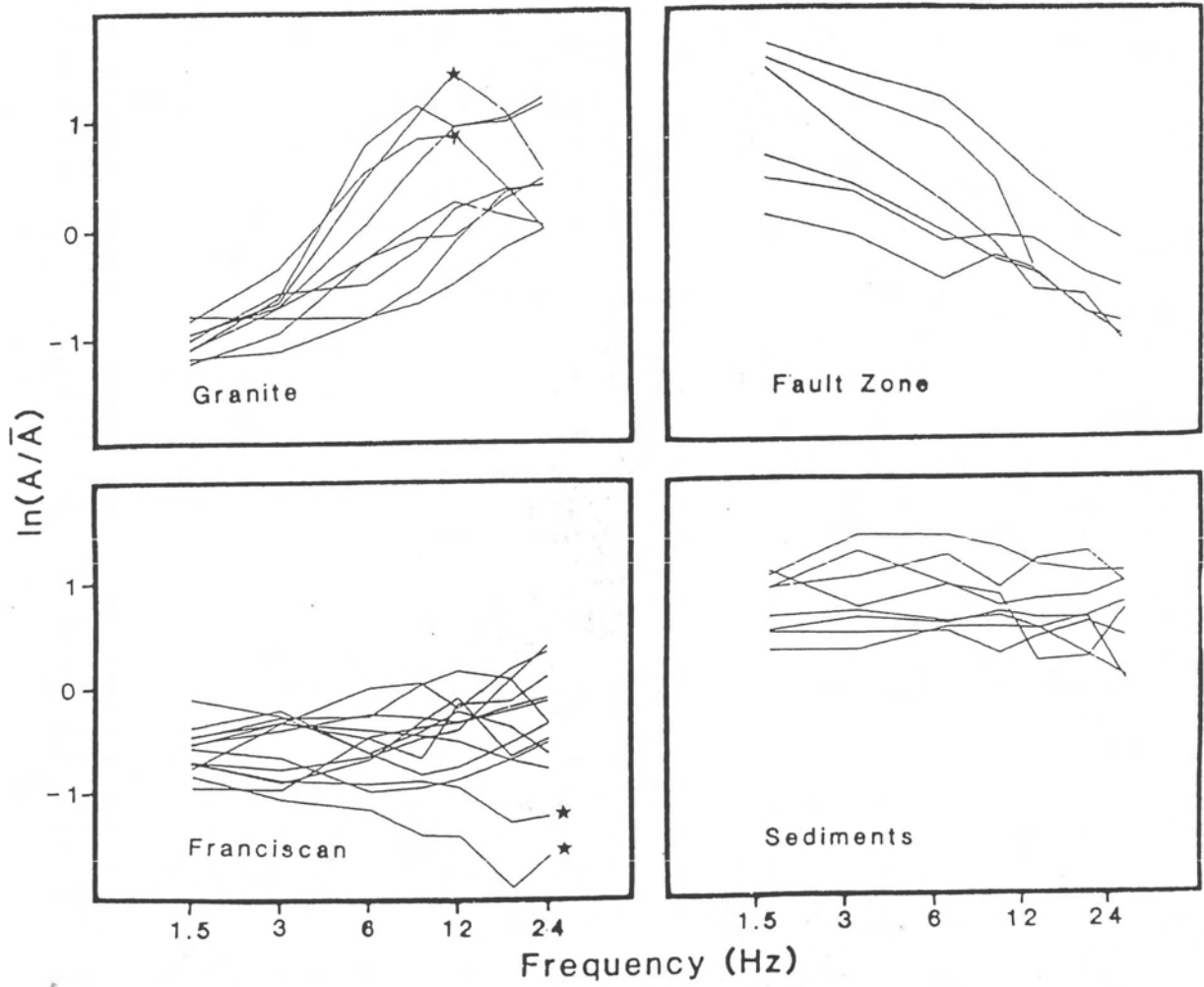


Fig. 2.22: Site response curve in the frequencies of various stations with different surface geologies [Phillips and Aki, 1986].

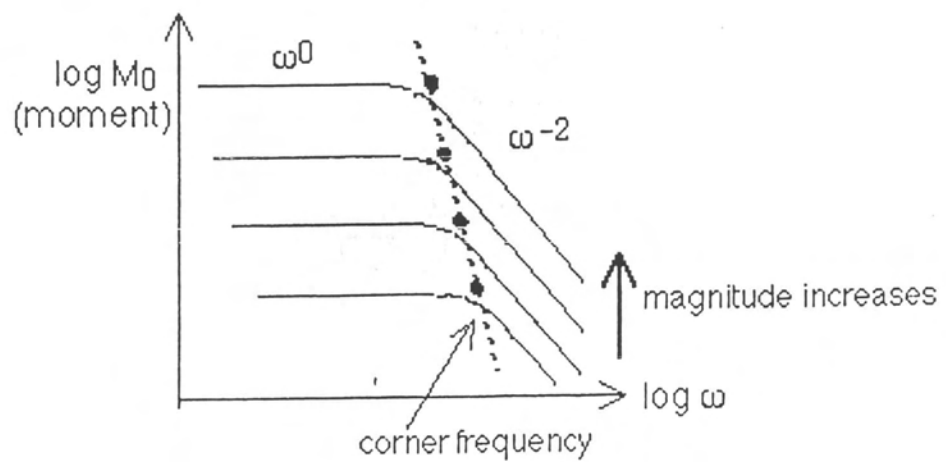


Fig. 2.23: Scaling law of seismic sources.

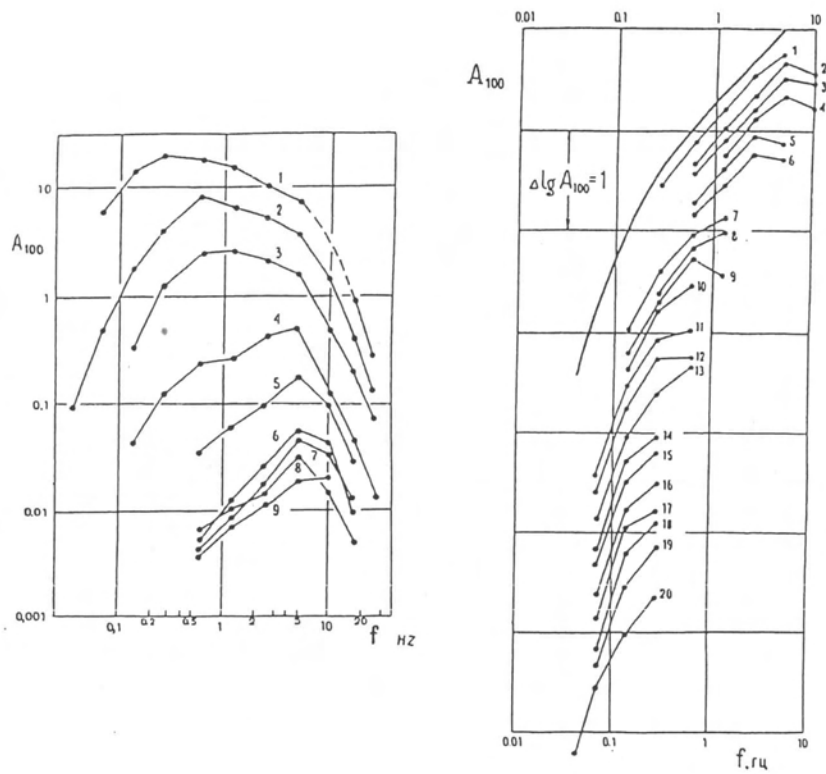


Fig. 2.24: Comparison of coda spectra and estimated source spectra with earthquakes of various sizes recorded in Garm [Rautian and Khalturin, 1978].

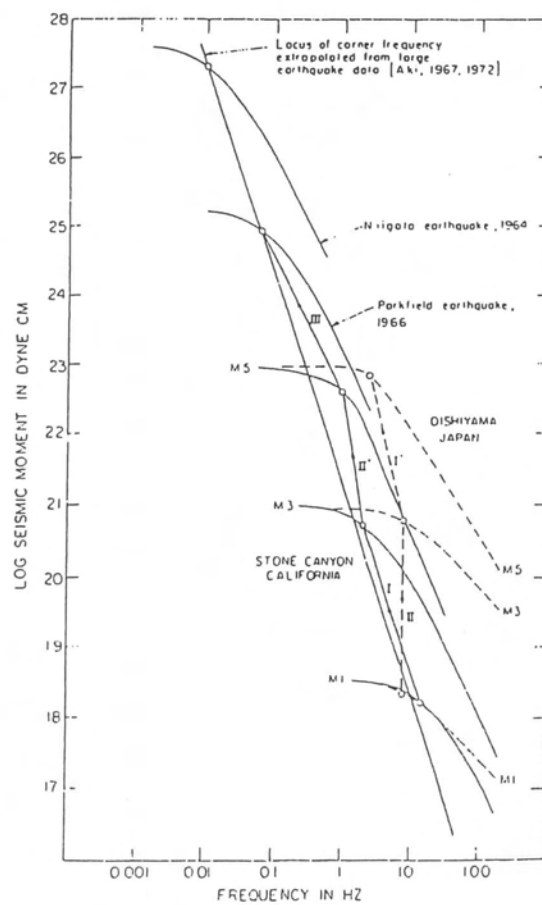


Fig. 2.25: Schematic source spectra estimated by coda waves recorded over the world [Aki and Chouet, 1975]. (Copyright by the American Geophysical Union)